

Elastic and inelastic processes in $H^+ + C_2H_6$ collisions below the 10-keV regime

Reiko Suzuki

Computer Center, Hitotsubashi University, Kunitachi, Tokyo 186-8601, Japan

Sachchida N. Rai

Computer Centre, Bijni Complex, North-Eastern Hill University, Shillong-793003, Meghalaya, India

Heinz-Peter Liebermann and Robert J. Buenker

Fachbereich C-Mathematik und Naturwissenschaften, Bergische Universität Wuppertal, D-42119 Wuppertal, Germany

Lukáš Pichl

Division of Natural Sciences, International Christian University, Osawa 3-10-2, Mitaka, Tokyo 181-8585, Japan

Mineo Kimura

Graduate School of Sciences, Kyushu University, Fukuoka 812-8581, Japan

(Received 20 July 2005; published 14 November 2005)

Charge-transfer processes in collisions of H^+ ions with C_2H_6 molecules are investigated theoretically below 10-keV collision energies within a molecular representation. Converged total as well as differential cross sections are obtained in this energy range within a discrete basis of electronic states computed by *ab initio* methods. The present collision system suggests that the combination of the Demkov-type and Landau-Zener-type mechanisms primarily governs the scattering dynamics for the flux exit from the initial channel. The present charge-transfer cross sections determined are found to agree very well with all available experimental data below a few keV, but begin to deviate above 3 keV, in which the present results slowly decrease, while measurements stay nearly constant. From the study of the electronic state calculation, we provide some information on fragmented species, which should help shed some light on the fragmentation mechanism and process of $C_2H_6^+$ ions produced after charge transfer. In addition, the vibrational effect of the initial target to charge transfer is examined.

DOI: [10.1103/PhysRevA.72.052710](https://doi.org/10.1103/PhysRevA.72.052710)

PACS number(s): 34.70.+e, 82.30.Fi, 34.50.-s

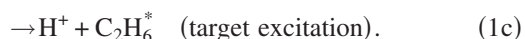
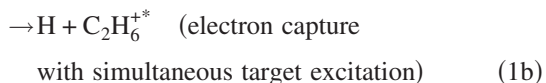
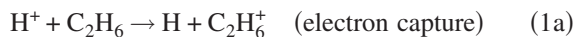
I. INTRODUCTION

Electron capture processes in collisions of ions with molecules in the low-keV-to-high-eV energy regions have remained relatively unstudied in research even though their importance is known in various applications from nanotechnology, and medical physics to atmospheric science and astrochemistry as well as other areas of basic sciences [1]. One of the primary reasons for this lagging progress in atomic and molecular physics lies in inherent complexities in treating molecular targets in both theory and in experimental analysis. Even for a relatively active research area such as chemical-reaction dynamics, the target species studied are quite limited and collision energies considered are quite narrow, normally within the low-eV region only. Despite these limited areas of study, however, based on our recent rigorous systematic investigations of ion-molecule collisions including those of H_2 target [2–5], numerous new interesting findings and understandings emerge which undoubtedly help to revise our previous views of collisions dynamics. These studies were partly stimulated by recent rapid developments in research areas such as fusion, plasma processing and ion-beam technology, and a proper theoretical understanding of dynamical aspects as well as the determination of accurate reaction cross-sections were urgently required in these applications.

We have initiated a series of rigorous theoretical studies of elastic and electron capture processes in the collisions of

H^+ ions with various molecules, primarily hydrocarbons, in the region below a few keV down to a few tens of eV. Hydrocarbon molecules are common under most environmental conditions, and are found to exist abundantly in various astrophysical and atmospheric environments. They are particularly versatile for fusion reactors, and plasma-chemistry atmospheres, which are known to play a crucial role in determining a number of physical effects [3]. Various kinds of hydrocarbons in sizable amounts have recently been found at the edge-plasma region in fusion reactors such as in divertors where carbon-faced materials are used, and the hydrocarbons produced are of concern since they play key roles as poisons in the reactor. Thus the knowledge of these hydrocarbons and their fragmented species is crucial for accurate determination of the carbon chemistry in fusion research. Therefore, we also examine the fragmentation processes and fragmented species produced based on the electronic states calculated. In this series of research on hydrocarbons, we have undertaken the study of H^+ -ion collisions with CH_4 [4], C_2H_2 [5], and C_2H_4 [6,7], in addition to C^+ -ion collisions with C_3H_4 [8]. These investigations have unearthed various new insights and effects, and showed the importance of isotopic, isomeric, steric and temperature effects, which were previously considered to be negligible in this collision energy domain. These findings have had a significant impact on various applications and have also stimulated careful reassessments of previous experimental studies.

In the present work in this series, a more complex system, the ethane molecule (C_2H_6) has been considered in order to study its scattering dynamics for electron capture and excitation and to examine its fragmentation products based on analysis of its dissociation reactions. This molecule is of the C_2H_m molecules studied, and is interesting for comparison of dynamics within this family. It is also of particular importance as an exit channel in the chain for production of larger hydrocarbons and hence, biomolecules. The processes studied are, in addition to elastic scattering,



We are concerned primarily with electron capture and direct elastic scattering in collisions of H^+ ions with C_2H_6 molecules for energies below 10 keV in order to elucidate scattering dynamics for a molecular target and to provide accurate cross-section values. Contribution from the process (1b), i.e., electron capture with simultaneous target excitation, is also examined. The products of process (1c) lie about 2.9 eV above the initial channel. There are several intermediate charge-transfer channels, and therefore, the contribution from the process (1c) is expected to be of negligible relevance in the present energy region.

We obtain our results by using a molecular orbital expansion method within a fully quantum-mechanical as well as a semiclassical formalism. For detailed examination of the collision dynamics, three molecular configurations are specifically considered for direct study: a proton approaches (i) parallel to, or (ii) perpendicular to the C—C axis in the molecular plane, and (iii) perpendicular to this plane.

Interferences of various origins are a key subject of fundamental interest in physics, and they also form an essential basis for possible use of this technique for material and surface analysis. Hence, these effects will be highlighted in the present investigation as well.

II. THEORETICAL MODEL

The theoretical methods employed are somewhat standard in our series of studies [4–9], so a summary of specific features for this particular system will be given in the present work.

A. Molecular electronic states

The adiabatic potential-energy curves and corresponding wave functions are calculated by means of the multireference single- and double-excitation configuration-interaction (MRD-CI) method [10–16], with configuration selection and energy extrapolation. The Table CI algorithm [13,14] is employed for efficient handling of Hamiltonian matrix elements for the many-electron basis functions (symmetrized linear combinations of Slater determinants).

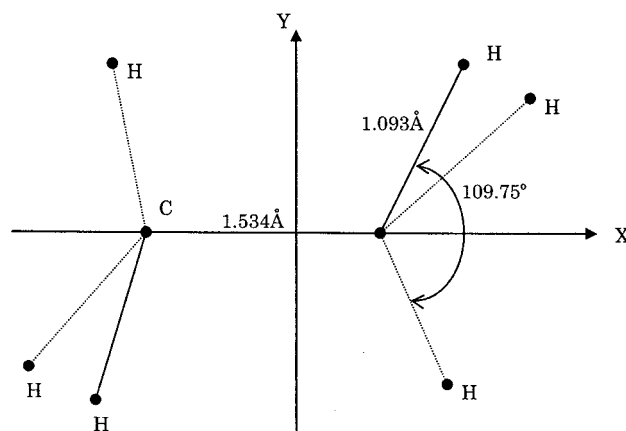


FIG. 1. Schematic diagram indicating the molecular axis orientation employed for the $[H+C_2H_6]^+$ collision system.

The atomic orbital (AO) basis set in the present calculations consists of contracted Cartesian Gaussian functions. For the carbon atoms a primitive basis ($10s, 5p, 2d, 1f$) contracted to $[4s, 3p, 2d, 1f]$ due to Dunning [17] is employed. From the same reference, a primitive basis ($5s, 2p, 1d$) contracted to $[3s, 2p, 1d]$ is used for the hydrogen atoms. Diffuse AOs with two s ($\alpha_s=0.023a_0^{-2}$ and $0.0055a_0^{-2}$), two p ($\alpha_p=0.021a_0^{-2}$ and $0.0049a_0^{-2}$), and one d ($\alpha_d=0.015a_0^{-2}$) exponents have been placed at the midpoint of the C—C bond. Altogether, the AO basis therefore consists of 189 contracted Gaussian functions.

The calculations are carried out in the C_2 and C_s point groups, taking into account the approach of the proton to the midpoint of the ethane molecule along the three principal axes. In the practical calculation of eigenvalues and eigenfunctions, all coordinates within the C_2H_6 molecule were frozen at the equilibrium intramolecular distances of the D_{3d} geometry [18]: $r_{C-C}=1.534$ Å, $r_{C-H}=1.093$ Å, and $\theta_{H-C-H}=109.75^\circ$. The C—C bond is located on the x axis with its midpoint at the origin of the coordinate system, and two of the H atoms lie in the XY plane while the others are placed symmetrically above and below it, as shown in Fig. 1.

The target molecular geometry is fixed at the equilibrium configuration of the neutral ground state [19] during collisions. This restriction is justified since the present collision time is much shorter, less than 10^{-17} s, than the relaxation time of 10^{-13} s, or longer. Hence, only the internuclear distance R between the H^+ projectile and the midpoint of the C—C bond was varied in the molecular-state calculations. The C—C bond is placed along the x axis with its midpoint at the origin of coordinate system, and the location of the C—H bonds is shown in Fig. 1. The incident projectile approaches the target from three different directions: (i) the proton moves on the x axis toward the C atom between the H—C—H bonds, (ii) the proton approaches the midpoint of the C—C bond on the y axis, and (iii) the proton moves along the z axis toward the midpoint of the C—C bond.

B. Scattering dynamics

Both fully quantum-mechanical and semiclassical approaches within a molecular representation have been em-

ployed, the so-called molecular-orbital close-coupling (MOCC) method. Accordingly, dynamical transitions are driven by nonadiabatic couplings [18].

The total wave function for scattering in a quantum mechanical approach is described as a product of the electronic and nuclear wave functions, while it is described as a product of a time-dependent coefficient with the electronic wave function in the semiclassical picture. Substitution of the total scattering wave function in a quantum mechanical approach into the stationary Schrödinger equation yields coupled, second-order differential equations for the nuclear wave functions. It is computationally convenient to solve the coupled equations in a diabatic representation [18]. The transformation from the adiabatic to the diabatic representation can be readily achieved by introducing a unitary transformation matrix $C(R)$. In this representation the nuclear wave function for the heavy particles is given by $X^d(R) = C^{-1}X^a(R)$, and the corresponding diabatic potential matrix is defined as $V^d = C^{-1}V^aC$, where V^a is the adiabatic potential matrix. The resulting coupled equations for $X^d(R)$ are thus given in much simpler form (see Ref. [8]). The coupled equations thus obtained are solved numerically to obtain the scattering S_ℓ matrix for each partial wave ℓ . The differential cross section as a function of scattering angle θ is then obtained from the standard formula by using the scattering S_ℓ -matrix element for partial wave ℓ and the momentum of the projectile. Analytical integration over all angles in the partial wave expansion gives the total scattering cross section, which are also independently obtained in the semiclassical framework.

In the semiclassical approach, the total wave function is substituted into the time-dependent Schrödinger equation, which yields a set of first-order coupled differential equations for the time-dependent coefficients. By solving it numerically, one can obtain the transition amplitudes. Integration of the square product of the amplitude over the impact parameter b weighted with b gives the desired cross sections.

In the present calculations we have carried out up to four-state close-coupling treatments. The corresponding molecular states arise from the initial [$H^+ + C_2H_6$], the electron capture [$H + C_2H_6^+$], the target excitation [$H^+ + C_2H_6^*$], and the charge transfer with excitation [$H + C_2H_6^{+*}$] channels. The differential cross sections are obtained in the quantal framework; partial and integral cross sections were also independently obtained with the semiclassical method. Two results by the semiclassical and quantal approaches are found to agree within 15% at the energy where they overlap.

III. RESULTS

A. Adiabatic potentials and couplings

Only specific points relevant to the collision dynamics discussed below are highlighted in the present work.

The adiabatic potentials for the present collision systems for three different nuclear configurations (i)–(iii), respectively, are shown in Figs. 2(a)–2(c) and corresponding representative radial coupling matrix elements are depicted in Fig. 3. The initial [$H^+ + C_2H_6$] state is the third from the

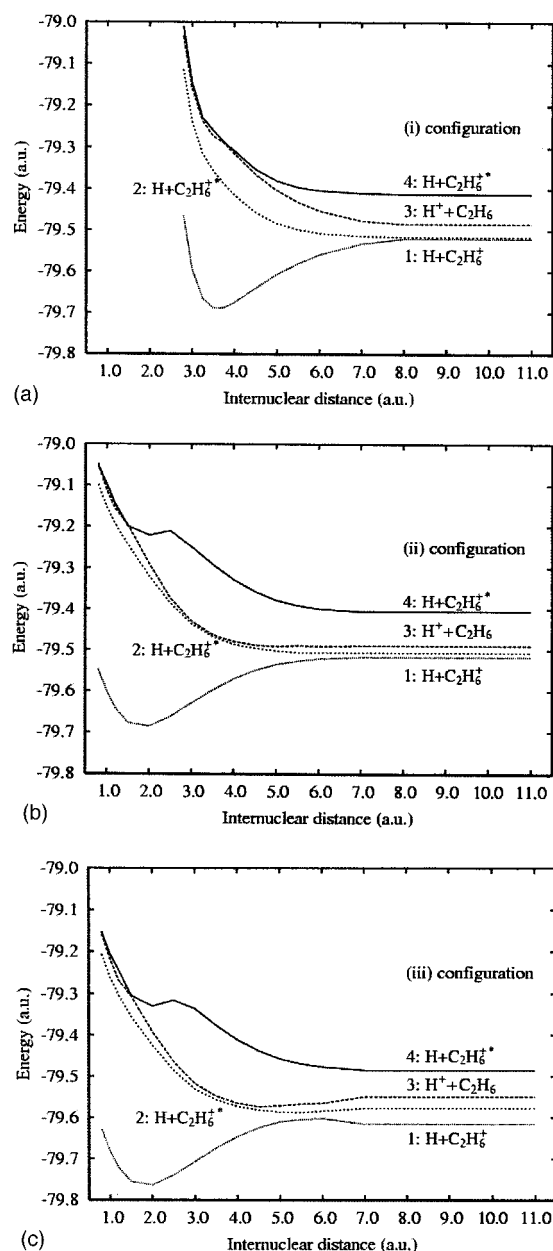


FIG. 2. The adiabatic potentials of the $[H + C_2H_6]^+$ system for the (a) (i), (b) (ii), and (c) (iii) directions (see text for definition) of approach of the proton.

bottom, while the lowest state corresponds to the ground [$H + C_2H_6^+$] state, that is, electron captured state and the second and the fourth correspond to electronically excited captured [$H + C_2H_6^{+*}$] states, i.e., capture+excitation. The valence electron in each of the states possesses σ character for all the nuclear configurations. As a result, all low-lying states have σ character, and hence, only radial couplings among them are the primary cause of the dynamics.

For all nuclear configurations, the initial and second states are close, and the initial and fourth states show rather parallel nature for all R , as the curves are repulsive except for the ground-state potential. For (i) configuration, the initial (third) and fourth states appears to possess weak and broad avoided

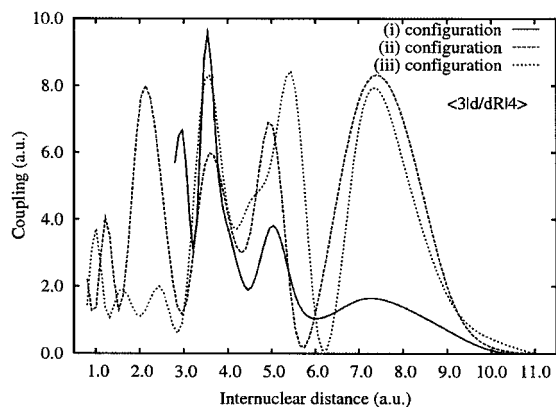


FIG. 3. Representative radial couplings between the initial and electron-capture states for all three configurations.

crossings at around $4a_0$, while for (ii) and (iii) configurations, the initial and the second states have a weak avoided crossing at around $3.5a_0$ and $3.0a_0$, respectively. Apart from these apparently localized avoided crossings, the potential energy curves do not show any hint of strong interactions but there remain relatively large values of nonadiabatic coupling at large distances. This suggests that a combination of the Landau-Zener-type and Demkov-type mechanisms for charge transfer is effective. As seen, three sets of adiabatic potentials are somewhat different. Hence, depending on the proton path taken, very different collision dynamics can be anticipated, that is, a strong steric effect. This feature will be considered in more detail below. Representative radial coupling matrix elements, which connect the initial and strong charge-transfer channels are shown in Fig. 3. It was checked in the calculation that addition of higher lying roots does not alter the results, as the radial couplings to the initial state are extremely weak. The manifold of four states considered here should thus accurately describe the electron capture dynamics. The ionization channel should play a considerable role at energies higher than 10 keV, but in the present energy region studied, the convergence within discrete manifolds should be reliable.

B. Differential cross sections

Differential cross sections (DCSs) for the (i), (ii), and (iii) nuclear configurations at 0.5 keV (left panel) and 1.5 keV (right panel), respectively, are shown in Figs. 4(a)–4(c) over the entire range of scattering angle. DCS angles up to 10° are also depicted separately in Figs. 5(a)–5(c) for the three configurations. Figure 6 shows the DCSs averaged over the three molecular configurations.

Direct elastic scattering processes are found to dominate in magnitude over electron capture for all cases at all energies and for most scattering angles. Beyond the scattering angle of 10° , the DCSs for (ii) and (iii) configurations show very weak angle independence up to roughly 170° . For the (i) configuration, however, electron-capture DCSs show weak angle dependency, and increase beyond 160° at 1.5 keV.

In order to examine this effect more clearly, we include s -matrix elements as a function of angular momentum ℓ for three configurations at 0.5 keV in Figs. 7(a)–7(c), respectively. For the (i) configuration, in addition to small but high-pitched oscillations, large gradual irregular oscillatory structures enveloped high-pitched oscillations can be seen, and these are most likely due to a multiple-scattering effect (see also the coupling in Fig. 3). This feature is quite different from those for atomic and symmetrical molecular cases where oscillatory patterns generally show more regular structures (see the H_2 case in Ref. [9]). The present oscillatory patterns for the (i) configuration do not similarly appear for the (ii) and (iii) molecular configurations, and are completely different. These are, again, a manifestation of the steric effect. This oscillatory structure indicates that the electron jumps back and forth between the projectile and target continuously and rapidly during a single collision, i.e., electron-capture and electron-loss continuously take place. In the asymptotic region of the collisions, the electron settles either on the direct elastic channel or electron-capture channel, hence there is interference between these two possibilities as a function of the collision energy and the impact parameter.

Since all three nuclear configurations exhibit similar magnitude for the DCSs as well as similar overall shape, the general features seen in the averaged DCSs (Fig. 6) are easily deduced from these three DCSs. This can be clearly noticed when DCSs in the region of 10° to 60° are examined. The sharp dip at around 90° in the (ii) configuration and several small dips in the (ii) and (iii) configuration disappear.

C. Partial cross sections

Partial cross sections are illustrated in Fig. 8 for formation of the ground as well as excited $C_2H_6^+$ ions after charge transfer for the three configurations. For the (i) configuration, the 1-state population becomes dominant above 0.2 keV, while the 2-state population is important below this energy, and the 1-state population becomes the weakest above 0.4 keV. For the (ii) configuration, the 1-state population is dominant in all energies over the other two. For the (iii) configuration, the 4-state population is dominant, while the 1-state population is the weakest in most of the energy range. The strong differences in capture dynamics observed above, which are an apparent steric effect, are suggestive of a different fragmentation mechanism and hence corresponding fragmented species produced.

The averaged values for the three configurations are shown in Fig. 9(a). For those values in the (i) configuration, the 1-state population becomes dominant above 0.2 keV, while the 2-state population is important below this energy, and the 2-state population becomes the weakest above 0.4 keV.

Averaged partial cross sections to the 4-state for the (i), (ii), and (iii) configurations averaged are shown in Fig. 9(b). The cross section for the (ii) configuration is the weakest in most of the energy range, because for this configuration, the projectile crosses through the region where the charge concentration is the lowest.

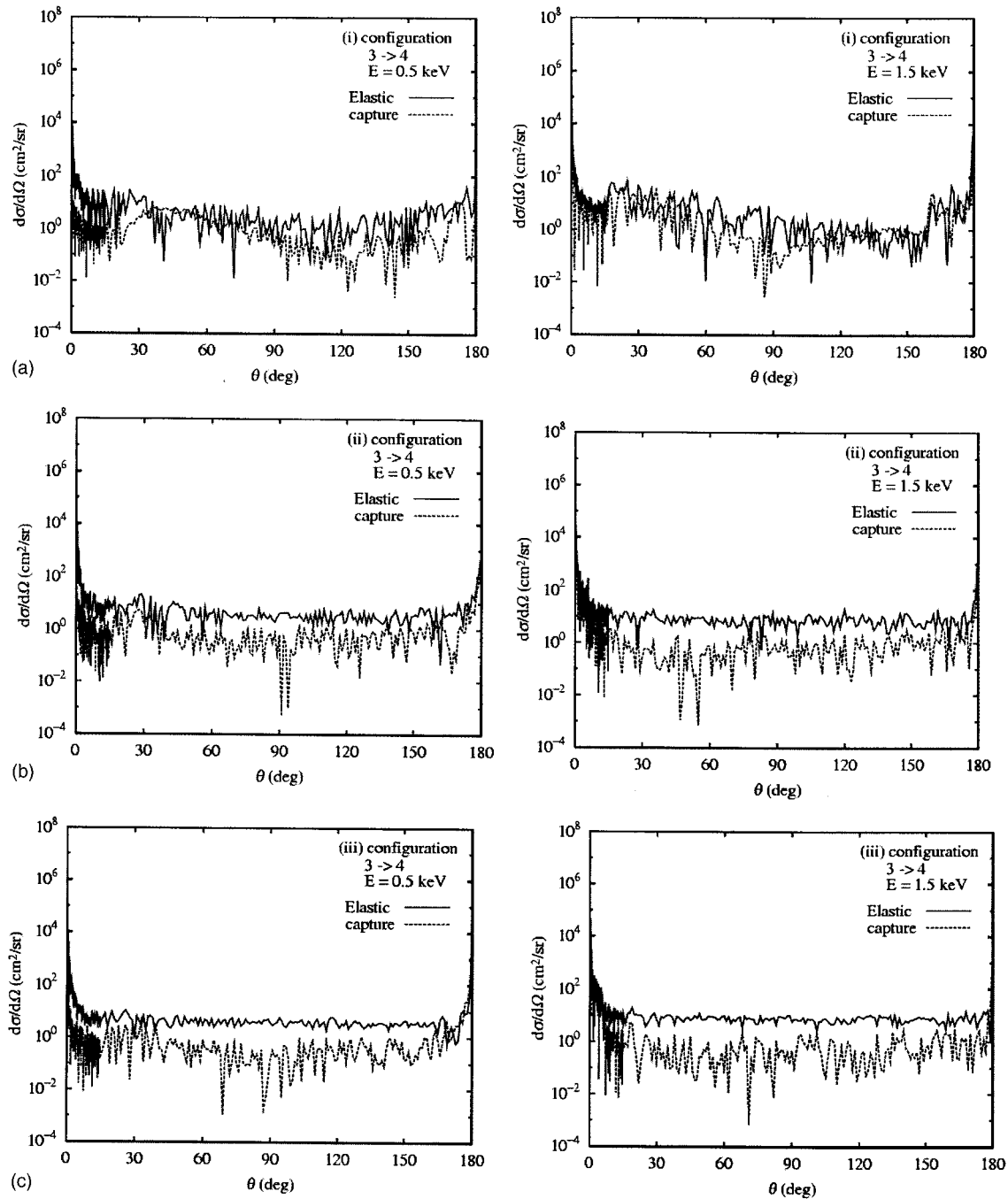


FIG. 4. Differential cross sections for the (a) (i), (b) (ii), and (c) (iii) configurations at 0.5 keV (left panel) and 1.5 keV (right panel) from the initial state 3 to the electron captured state 4. Solid line, direct elastic scattering; dashed line, electron capture.

D. Cross sections for total capture and capture+excitation processes

The sum of all electron-capture cross sections for each of three configurations separately is shown in Fig. 10(a) from 0.1 keV to 10 keV, and the total cross sections averaged over all three configurations [process (1a)+(1b)] and electron capture with simultaneous target excitation (process (1b)) are included in Fig. 10(b). For comparison, these total cross sections are again displayed in Fig. 11 along with a theoretical estimation by Janev *et al.* [20] and observed results by Kusakabe *et al.* [7].

As is apparent, the total cross sections for the (ii) configuration are smallest, while those for the (i) configuration are largest among the others in the energy range studied, and the results for the (iii) configuration lie between them. All three cross sections, however, display a similar energy dependence. [Capture+excitation] shows a similar energy dependence as the total, but smaller by 40% in the entire energy region.

Janev *et al.* [20] proposed an analytical formula by fitting charge transfer cross sections of $H^+ + C_nH_m$ collisions based on the Demkov approximation through evaluating existing

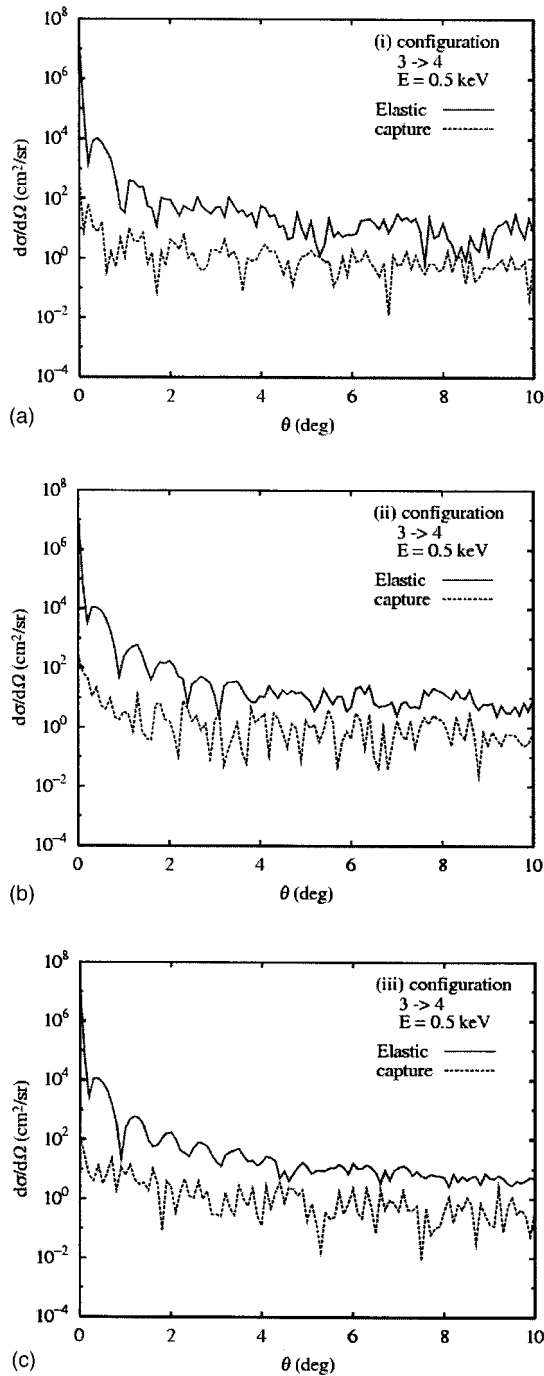


FIG. 5. Differential cross sections for small scattering angles up to 10° at 0.5 keV from the initial state 3 to the electron capture state 4 are shown. Solid line, direct elastic scattering; dashed line, electron capture.

sets of experimental data. This formula has also been employed for interpolation and extrapolation in the analysis of a large volume of experimental data by his group and they have claimed that the analytical formula is able to reproduce experimental results within an order of magnitude at 10 keV/u. For the lower energy-side from 0.1 to 1 keV/u, they determined the parameters for the formula by simply fitting the data by Toburen *et al.* [21]. At higher energy above

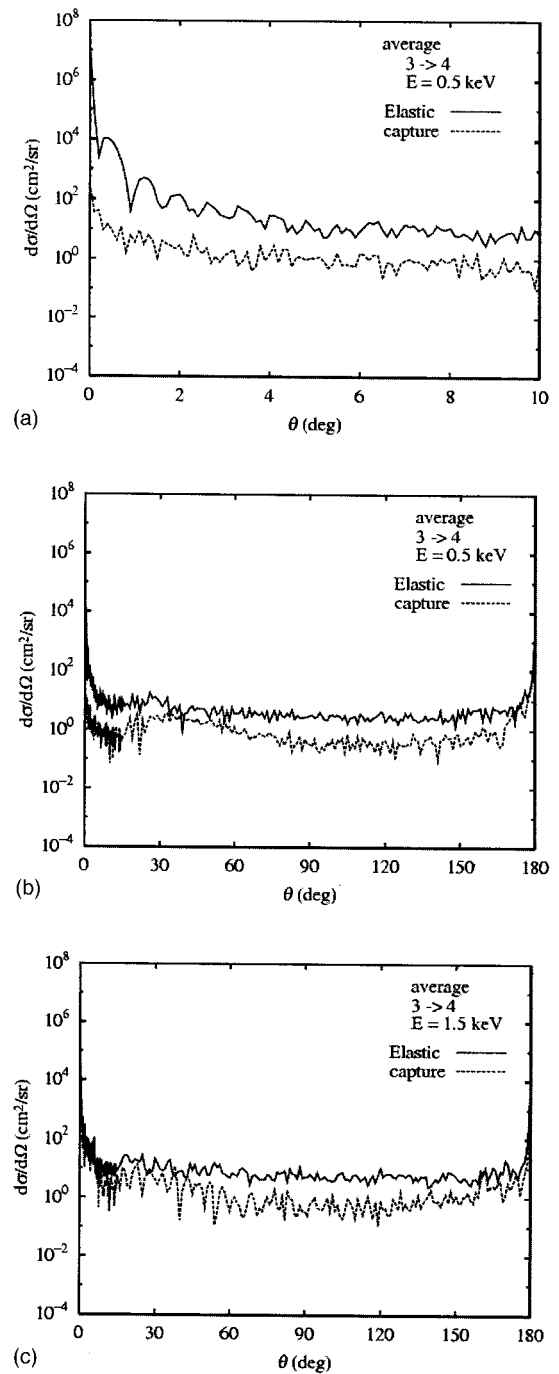


FIG. 6. Differential cross sections averaged over three configurations.

60 keV, Sanders *et al.* [22] experimentally investigated charge-transfer processes. Although there is no overlap in the energy region studied between the present results and those of Sanders *et al.*, the extrapolation of our results appears to tie in reasonably well with theirs.

Kusakabe *et al.* [7] have recently investigated charge-transfer processes experimentally from 0.2 keV to 4 keV for various targets of hydrocarbons including the present C_2H_6 molecules. Their results for the cross section were found to decrease monotonically as the collision energy increases,

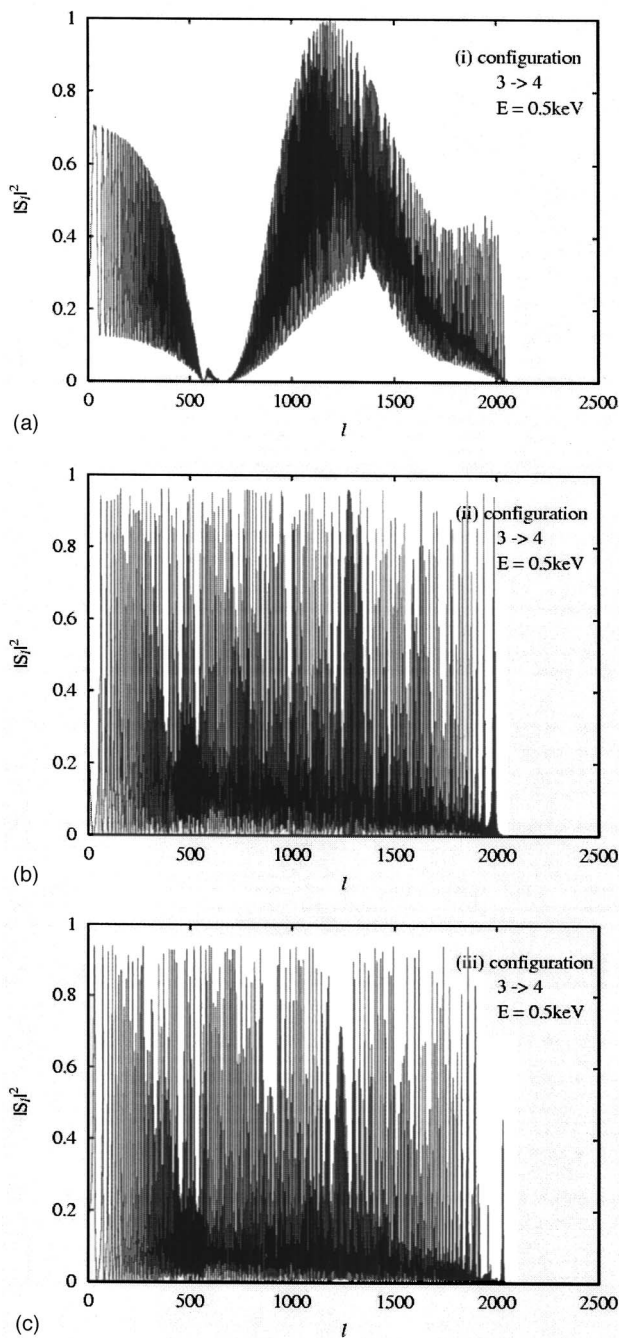


FIG. 7. S-matrix elements for three configurations.

with a value of $4 \times 10^{-15} \text{ cm}^2$ at 0.2 keV to $2.2 \times 10^{-15} \text{ cm}^2$ at 4 keV.

Generally, all results are found to agree very well, giving similar magnitude and energy dependence of the cross section below around 2 keV. The results begin to deviate as the energy increases. Janev's and Kusakabe's results appear only to decrease rather slowly in the entire energy region studied, while the present results drop rather sharply above 3 keV/u. Note that the results by Janev *et al.* were determined based on those of Kusakabe *et al.* [7], and hence their results are nearly identical. The results by Janev and Kusakabe's are found to be larger by a factor of 2 than our result at above 3 keV. By inspecting the nature of adiabatic potential

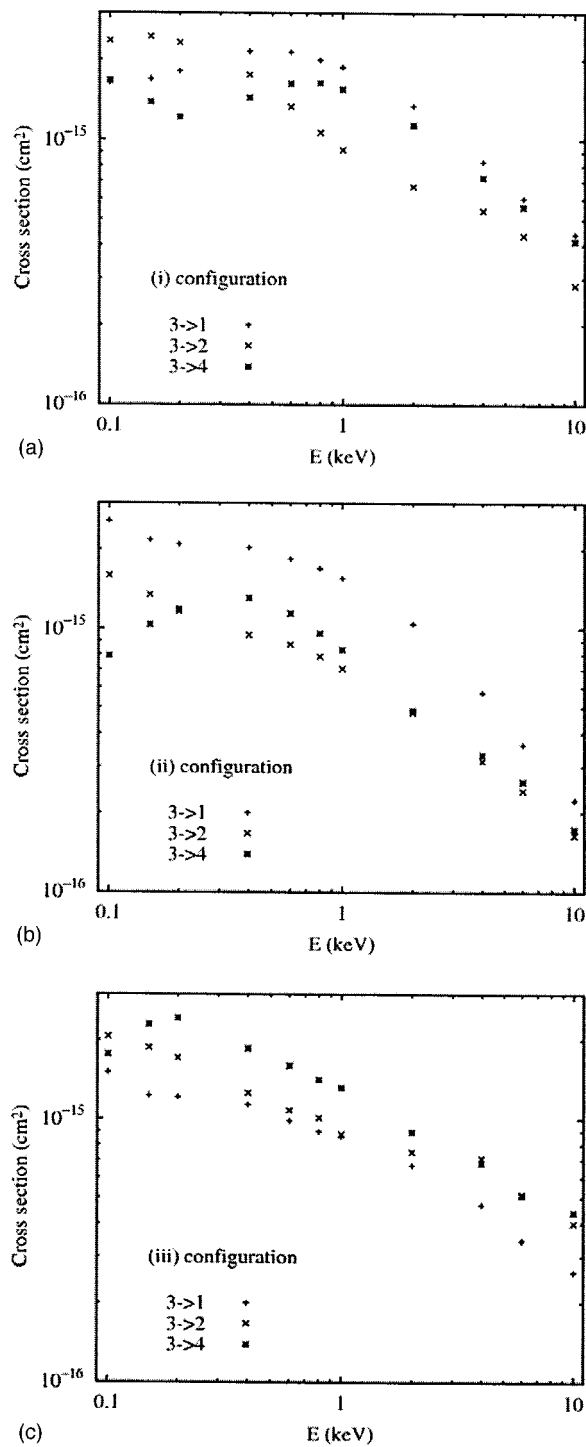


FIG. 8. Partial cross sections from each channel for the (i), (ii), and (iii) molecular configurations.

curves and corresponding couplings, it may be more plausible to believe the decrease at higher energies. However, it is also possible to consider that this small difference may correspond to the increasing relative importance of higher excited charge-transfer channels we ignored in the present calculation.

The analytical formula by Janev *et al.* provides us with a useful guideline for fitting experimental data in the two-state Demkov approximation. The cross section difference arising

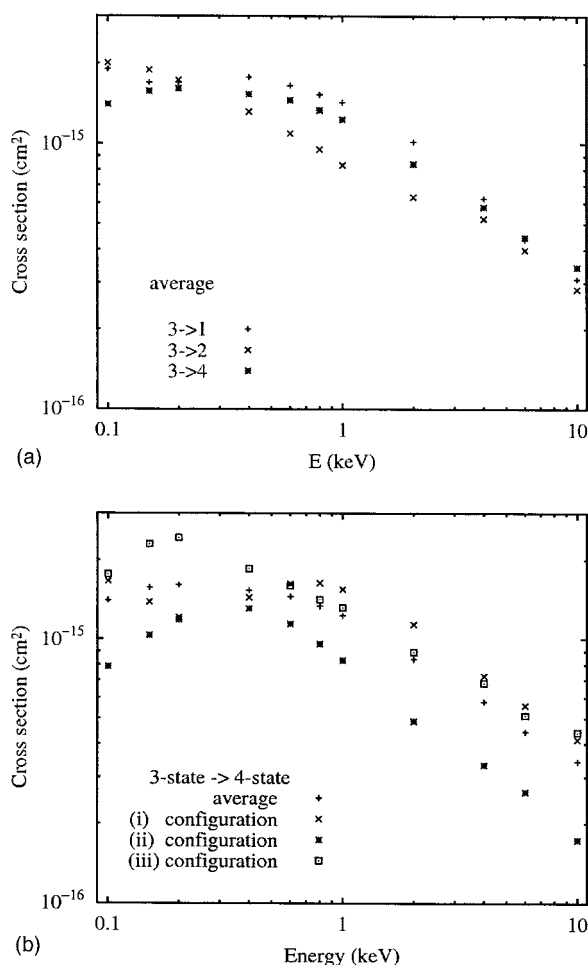


FIG. 9. (a) The averaged partial cross sections for the 1, 2, and 4 state populations. (b) Partial cross sections from 3 state to 4 state for (i), (ii), and (iii) configuration.

in the present case is attributed to the multi-channel character of electron capture (cf. the three capture states considered in Fig. 2) and the combination of Landau-Zener (LZ) and Rosen-Zener-Demkov (RZD) type of transitions, and it remains within the order of accuracy claimed in Ref. [20].

E. Vibrational effect

Vibrational energies of C₂H₆ are known to be from the lowest (in cm⁻¹): 289, 822, 995, 1190, 1379, and many more for twisting, bending, symmetric and asymmetric stretching modes [23]. At room temperature, a sizable fraction of vibrational excited states is expected to be present in the experiment, and hence their effect for charge transfer should be tested carefully in order to make a sound analysis of the experimental results. We have also estimated charge transfer from the vibrationally excited target. As seen from the adiabatic potential curves in Figs. 2(a)–2(c), as the vibrational level increases, the energy gap between the initial and the dominant charge transfer state widens, making the transition to this level less favorable. The gap between the initial and the second charge transfer state, however, decreases, making the transition slightly favorable, hence compensating

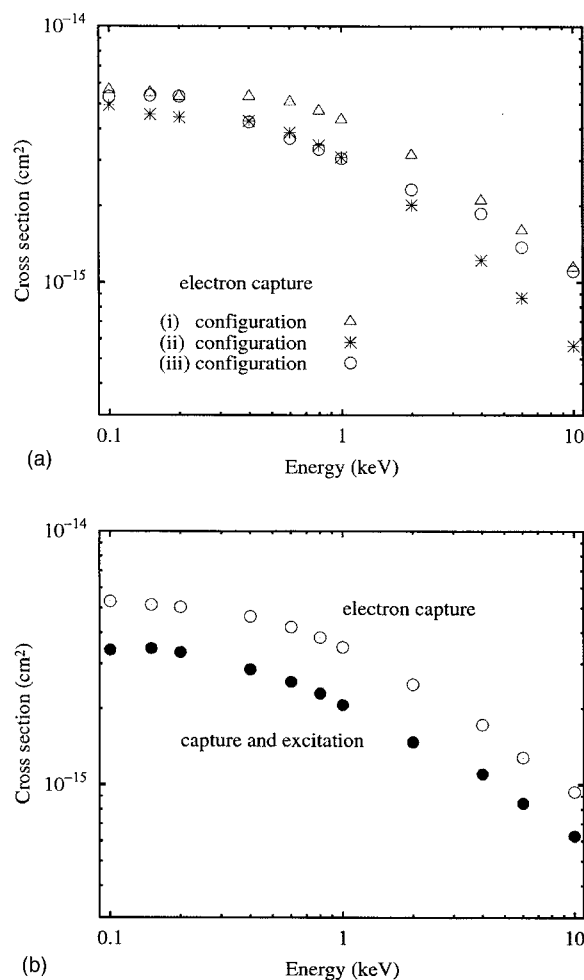


FIG. 10. (a) Total electron-capture cross sections of the H⁺ + C₂H₆ collisions averaged over (i), (ii), and (iii) configurations. (b) [Electron capture+excitation] cross sections of the process (1b).

the loss of the previous process. Therefore, the net change of charge transfer is not large in this collision energy region in terms of the vibrational state the target occupies initially. However, as the collision energy decreases to the low-eV regime, then, which vibrational level the target is in plays a significant role for determining the collision dynamics and hence cross sections.

F. Comparison of capture cross sections with CH₄, C₂H₂, C₂H₄, C₂H₆, and C₃H₈

In order for us to examine a possible relationship between the magnitude of electron-capture cross section and molecular quantities such as the number of total atoms in hydrocarbons, or the number of valence electrons in a molecule, we have plotted the cross sections as a function of the number of atoms in the molecule in Fig. 12, including our previous electron-capture cross-section data for CH₄, C₂H₂, C₂H₄ and C₃H₈ below 10 keV. At the lower-energy side, the order of the cross sections is clearly apparent as: C₃H₈ > C₂H₆ > CH₄ > C₂H₄ > C₂H₂. This is suggestive that the magnitude of the cross section depends on the number of atoms in a molecule or the molecular size, except for the case of CH₄.

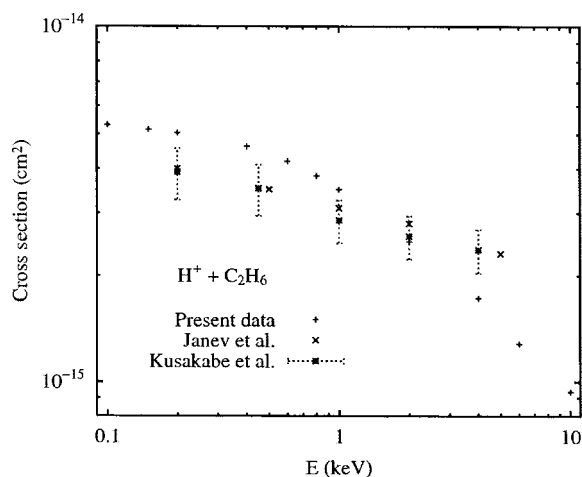


FIG. 11. Total electron capture cross sections of the H^+ + C_2H_6 system along with the estimates by Janev *et al.* and the observed data by Kusakabe *et al.*

The cross section for CH_4 is larger than that of both C_2H_4 and C_2H_2 , but slightly smaller than C_2H_6 and thus is somewhat irregular in this respect. The origin of this feature may arise from the nature of the bonding: C_2H_2 , C_2H_4 , and C_2H_6 have a triple, double and single bond, respectively, and for these hydrocarbons the major portion of the charge distribution depends on the nature of this C—C bonding. Therefore, as the bonding order increases, the more the electron distribution is concentrated in the C—C bond and becomes localized within a narrow spatial region, thus causing a smaller geometrical size and hence reducing the effective scattering region, as reflected in the sizes of the cross section for these three hydrocarbons. Since CH_4 has only four single bonds with each hydrogen atom, the charge distribution is somewhat more broadly spread out compared to its counterparts with double and triple bonds, thus increasing the effective size of the molecule and hence increasing the similarity with the C_2H_6 molecule. The C—H bond lengths for CH_4 , C_2H_2 , C_2H_4 , and C_2H_6 are 1.094, 1.058, and 1.086, 1.094 Å, re-

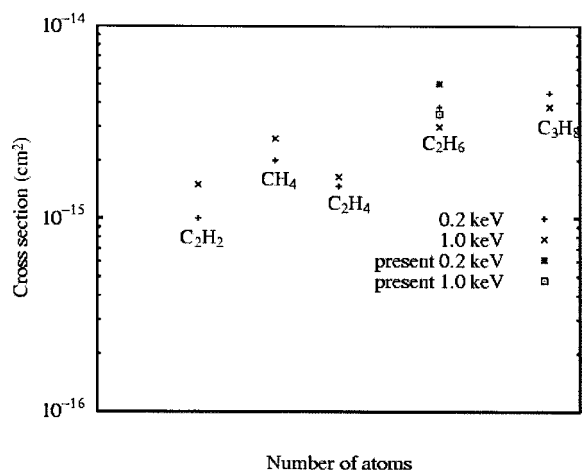


FIG. 12. Total cross sections as a function of the number of atoms in the molecule at specific energies as shown.

spectively, and the bond lengths for CH_4 and C_2H_6 are comparable to each other, but longer than the other two. Indeed, as pointed out above, the cross section for CH_4 is only slightly smaller in magnitude than that of C_2H_6 , where C_2H_6 contains only single bonds and hence may be rather similar in spatial charge distribution to CH_4 . The ionization potentials are known to be 12.51, 11.4, 10.5, and 11.52 eV, respectively [23]. Hence, the magnitude of ionization potential does not appear to correlate closely with that of the cross-section size, at least in this range of collision energy. Note that the ionization potential for CH_4 is the highest among them.

At higher energy above 3 keV or so, the differences in size of the cross section of the various molecules become much narrower because of the increasingly shorter interaction time, making it less sensitive to the individual physical characteristics of each molecule, but rather making a binary collision increasingly important.

G. Fragmentations

The calculations discussed above have been carried out with the ethane molecule frozen in its ground state equilibrium geometry. The collision energies considered are large enough to induce decomposition of the target system, however, and thus it is interesting to consider possible fragmentation channels. The C—C bond dissociation energy is 3.64 eV [24], and leads to a pair of methyl (CH_3) radicals in their planar equilibrium conformations. The lowest excited state of the product system is Rydberg $3s$ in character, lying 5.73 eV above the ground state, and it also prefers a planar geometry. Dissociation of one of the ethane C—H bonds requires somewhat more energy, 4.21 eV. It is more difficult to break the C—H bonds in the methyl radical after it has been formed (4.90 eV). The product in this case, methylene (CH_2), has a triplet ground state with a fairly large bond angle (134°). It also has a low-lying singlet state with a notably smaller equilibrium angle of 105° . The fragmentation of methylene has already been discussed in earlier work [6]. The C—H bond energy for methylene is 4.2 eV. When more than one H atom is removed from ethane, 2.24 eV/u can be retrieved through formation of H_2 molecules.

IV. SUMMARY AND CONCLUSIONS

Electron capture from C_2H_6 molecules by proton impact from a few tens of eV to about 10 keV has been investigated theoretically and accurate cross sections for the capture process as well as excitation are provided. The present cross-section results are found to be in reasonably good accord with those determined by Janev *et al.* based on their approximation up to 2 keV. Above this energy, the approximate cross sections stay nearly a constant, while the present results begin to decrease. Because of the combined RD and LZD type electron capture dynamics it may be unlikely that the cross section remains flat as the energy increases above a few tens of keV.

The main fragmentation products after ionization or electronic excitation are the methyl and methylene radicals ob-

tained by breaking the relatively weak C—C single bond of ethane.

ACKNOWLEDGMENTS

This work was supported in part by the Grant-in-Aid from the Ministry of Education, Science, Sport, Culture and Technology, Japan-Germany Collaborative Research Program of Japan Society for Promotion of Science (JSPS), Cooperative

Research Grant from National Institute for Fusion Science, Japan (R.S., L.P., M.K.), and Academic Frontier Program (L.P.). The financial support of the Fonds der Chemischen Industrie and the Deutsche Forschungsgemeinschaft (Grant Bu: 450/7-3) is gratefully acknowledged (R.J.B., H.P.L., and S.N.R.). One of us (S.N.R.) thanks the North-Eastern Hill University, Shillong, India, for granting a study leave to him at the University of Wuppertal during the course of the present work.

-
- [1] E. W. McDaniel, J. B. A. Mitchell, and M. E. Rudd, *Atomic Collisions* (Wiley Interscience, New York, 1993).
- [2] B. H. Bransden, and C. J. Joachain, *Ion-Atom Collisions* (Oxford University Press, New York, 1993).
- [3] H. Tawara, Y. Itikawa, H. Nishimura, H. Tanaka, and Y. Nakamura, *At. Plasma-Mater. Interact. Data Fusion* **2**, 41 (1992).
- [4] M. Kimura, Y. Li, G. Hirsch, and R. J. Buenker, *Phys. Rev. A* **52**, 1196 (1995).
- [5] M. Kimura, Y. Li, G. Hirsch, and R. J. Buenker, *Phys. Rev. A* **54**, 5019 (1996).
- [6] R. Suzuki, S. N. Rai, H.-P. Liebermann, R. J. Buenker, L. Pichl, and M. Kimura, *Phys. Rev. A* **71**, 032710 (2005).
- [7] T. Kusakabe, K. Asahina, A. Iida, Y. Tanaka, Y. Li, G. Hirsch, R. J. Buenker, M. Kimura, H. Tawara, and Y. Nakai, *Phys. Rev. A* **62**, 062715 (2000).
- [8] T. Kusakabe, K. Asahina, J. P. Gu, G. Hirsch, R. J. Buenker, M. Kimura, H. Tawara, and Y. Nakai, *Phys. Rev. A* **62**, 062714 (2000).
- [9] T. Kusakabe, M. Kimura, L. Pichl, R. J. Buenker, and H. Tawara, *Phys. Rev. A* **68**, 050701(R) (2003); **70**, 052710 (2004).
- [10] R. J. Buenker and S. D. Peyerimhoff, *Theor. Chim. Acta* **35**, 33 (1974).
- [11] R. J. Buenker and S. D. Peyerimhoff, *Theor. Chim. Acta* **39**, 217 (1975).
- [12] R. J. Buenker, *Int. J. Quantum Chem.* **29**, 435 (1986).
- [13] R. J. Buenker, in *Proceedings of the Workshop on Quantum Chemistry and Molecular Physics, Wollongong, Australia*, edited by P. Burton (University Press, Wollongong, 1980); R. J. Buenker and R. A. Phillips, *J. Mol. Struct.: THEOCHEM* **123**, 291 (1985).
- [14] S. Krebs and R. J. Buenker, *J. Chem. Phys.* **103**, 5613 (1995).
- [15] R. J. Buenker, D. B. Knowles, S. N. Rai, G. Hirsch, K. Bhannuprakash, and J. R. Alvarez-Collado, in *Studies in Physical and Theoretical Chemistry*, edited by R. Carbo (Elsevier, Amsterdam, 1989), Vol. 62, p. 181.
- [16] D. B. Knowles, J. R. Alvarez-Collado, G. Hirsch, and R. J. Buenker, *J. Chem. Phys.* **92**, 585 (1990).
- [17] T. H. Dunning, Jr., *J. Chem. Phys.* **98**, 1007 (1989).
- [18] M. Kimura and N. F. Lane, in *Advances in Atomic, Molecular and Optical Physics*, edited by D. R. Bates and B. Bederson (Academic, New York, 1989), Vol. 26, p. 79.
- [19] *Interatomic Distances Supplement*, Special Publication No. 18, The Chemical Society, Burlington House, London, W1 (1965).
- [20] R. K. Janev, J. G. Wang, and T. Kato, NIFS-DATA-64, 2001.
- [21] L. H. Toburen, Y. Nakai, and R. A. Langley, *Phys. Rev.* **171**, 114 (1968).
- [22] J. M. Sanders, S. L. Varghese, C. H. Fleming, and G. A. Soosai, *J. Phys. B* **36**, 3835 (2003).
- [23] D. R. Lide, *CRC Handbook of Chemistry and Physics* (CRC Press, Boca Raton, FL, 2000).
- [24] G. Herzberg, *Electronic Spectra of Polyatomic Molecules* (Van Nostrand, New York, 1966).